Analyzing Electromagnetic Structures With Curved Boundaries on Cartesian FDTD Meshes

Yang Hao and Chris J. Railton, *Member, IEEE*

Abstract— In this paper, a new finite-difference time-domain (FDTD) algorithm is investigated to analyze electromagnetic structures with curved boundaries using a Cartesian coordinate system. The new algorithm is based on a nonorthogonal FDTD method. However, only those cells near the curved boundaries are calculated by nonorthogonal FDTD formulas; most of the grid is orthogonal and can be determined by traditional FDTD formulas. Therefore, this new algorithm is more efficient than general nonorthogonal FDTD schemes in terms of computer resources such as memory and central processing unit (CPU) time. Simulation results are presented and compared to those using other methods.

Index Terms—Algorithms, FDTD methods.

I. INTRODUCTION

IT IS WELL known that the finite-difference time-domain (FDTD) method that was put forward by Yee [1], has been proven to be a very efficient numerical algorithm in computational electromagnetics. However, the traditional FDTD algorithm is based on a Cartesian coordinate system, and it is difficult to exactly generate meshes for electromagnetic structures with curved boundaries. It is usual to utilize a staircase approximation into an FDTD method for curved structures and an accurate solution can only be obtained using very fine grids and, consequently, a very small time step. Moreover, it has been proven by Cangellaris and Wright [2], that numerical dispersion is caused by the use of a staircase mesh and, in computation of microwave resonators, studies have shown that the staircase approximation will underestimate the resonant frequencies and predict the Q factors which are lower than they are in reality. It is also difficult to precisely determine the radar cross section for a complex scatterer using this method.

Apart from the staircase approximation, there are three different commonly used types of the FDTD method which have been put forward to analyze electromagnetic structures with curved boundaries: The contour path algorithm [3]–[6], formulas in the curvilinear coordinate system [9], and the nonorthogonal FDTD method [7], [10]–[12]. In addition, the problem has also been addressed using a hybrid finite-volume finite-difference approach [13]. The contour path FDTD (CPFDTD) algorithm is based on the integral form of Ampere's and Faraday's Law. Formulas must be modified in those distorted cells which are near the curved boundaries. This is easy for curved perfect conductors because the tangential components of the electric field on the boundaries are zero. For dielectric objects where the tangential E field is nonzero, additional equations are needed to calculate the tangential components of the electric field from the equation of Ampere's Law. Although good results have been obtained by Jurgens *et al.* [3], [4], there are some shortcomings which include difficulties in generating the mesh. It has also been shown that in some cases the basic CPFDTD method is unstable. Modifications have been proposed which guarantee the stability of the scheme and facilitate simple generation of the distorted grids [5], [6].

The nonorthogonal FDTD algorithm was put forward by Holland [7] in 1983 and refined by many researchers including Fusco [10] and Mittra [11]. The underlying mathematics dealing with geometry and its application to electromagnetic fields can be found from [8]. Many numerical results have been obtained successfully in [9]–[11]. However, compared with the conventional FDTD scheme, two additional equations are needed in each iteration step in order to realize the transform between the contravariant and covariant components of electric and magnetic fields. Moreover, extra computer memory is needed to store the metric tensor of both E and H nodes, which are essential parameters in nonorthogonal coordinate systems. Therefore, the method is limited to relatively small structures. Although the nonorthogonal FDTD scheme is a generalized method, it is difficult to make it compatible with existing FDTD software which is based on the Cartesian coordinate system. In order to take advantage of the nonorthogonal FDTD algorithm, which is powerful for the computation of structures with curved boundaries, we use the theory of the nonorthogonal FDTD scheme within an underlying Cartesian coordinate system. In the combined method, most of the grid is in the Cartesian coordinate system with only those cells near the curved boundaries being treated as nonorthogonal cells. This new approach on FDTD has the following advantages.

1) A Cartesian grid is used for the majority of the problem space.
2) No special formulas are needed for curved boundaries.
3) There is little approximation in the formulations compared with the CPFDTD.
4) Less central processing unit (CPU) time and memory is needed than FDTD in nonorthogonal grids.
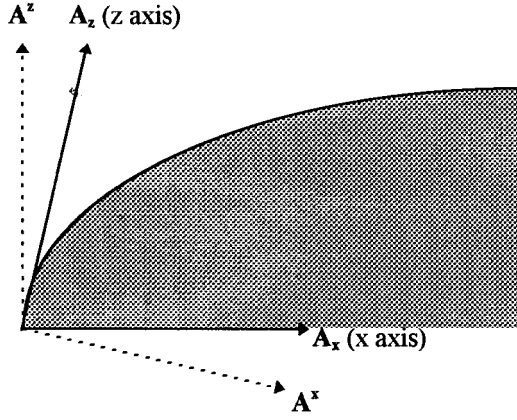
Fig. 1.   An arbitrary vector determined by other vectors.

Fig. 2.   Some cases of a curve splitting a Cartesian FDTD grid.

Fig. 3.   A "flag" cell extends to the neighbor cells.

an orthogonal coordinate system. No extra memory is needed to store the metric tensors and contravariant or covariant components. Only the values of those parts of the mesh which are close to the material boundaries are stored:

$$
\begin{aligned}
g_{ij} &= \vec{A}_i \bullet \vec{A}_j = |a_i a_j| \cdot \cos \theta_{ij} \\
&= |a_i a_j| \cdot \delta_{ij}, \qquad \text{if } \vec{A}_i, \vec{A}_j \text{ are orthogonal} \\
\delta_{ij} &= \begin{cases} 1, & i = j \\ 0, & i \neq j \end{cases}
\end{aligned} \tag{1}
$$

where θ_{ij} is the angle between two generalized axes, which is easy to obtain when these axes are straight lines, otherwise, the angle can be obtained from their tangential lines.

III. GENERATION OF THE MESHES

A. The Definition of "Flag" and "Triangle" Meshes

When allowing an arbitrary curve pass through a standard FDTD cell, the original cell is bisected. Some cases of this bisection are shown in Fig. 2.

Supposing an object has a curved boundary described as $z = f(x)$, then the intercepted points will be

$$
\begin{aligned}
&\text{intercepted with } z \text{ axis} \quad [m\delta x, f(m\delta x)] \\
&\text{intercepted with } x \text{ axis} \quad [f^{-1}(n\delta z), n\delta z]
\end{aligned}
$$

where m, n are the number of nodes, δx, δz are the space steps in FDTD, and $f^{-1}(z)$ is the inverse function of $f(x)$.

The first two types of cells in Fig. 2(a) and (b) are called "flag." In this case, the original cell is split by the material boundary into two cells which are still quadrilateral. We extend the neighboring cell (as shown in Fig. 3) and replace the E_x or E_z node by a E_t node on the material boundary.

The second type of cell, which is shown in Fig. 2(c)–(e) and is called "triangle," cannot be treated as FDTD cells directly—the mesh needs to be reconstructed such that all the cells are quadrilateral. To do this, an additional point is defined on the material boundary, such as C' in Fig. 4, and the edges
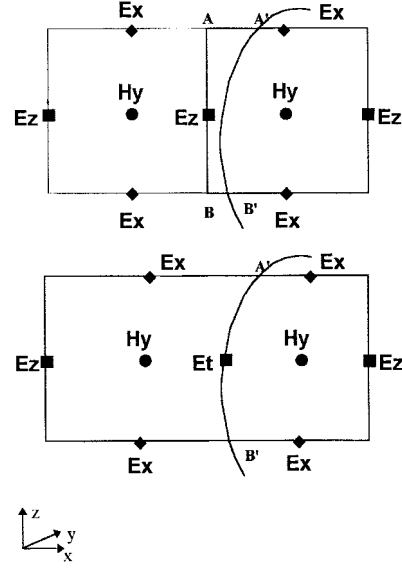
5) The approach is readily extended to dielectric boundaries.

The effectiveness of the new approach will be proven by some computational examples on determining the cutoff frequencies of both circular and rectangular perfect electric conductor (PEC) waveguides. The numerical results will be presented and compared with theoretical data and results from other methods.

II. A BRIEF DESCRIPTION OF THE NEW METHOD

As discussed in the previous section, the shortcomings of nonorthogonal FDTD are increased computational resources and the difficulty of generating irregular meshes. If we use Cartesian meshes and deal with most of the cells using in conventional FDTD, but use nonorthogonal FDTD near the oblique surfaces, the required computational resources will be reduced and the calculation of a much more precise solution for the curved objects will be facilitated.

The metric tensor can be obtained from $g_{ij} = \vec{A}_i \bullet \vec{A}_j$, where $\vec{A}_i$, $\vec{A}_j$ are bases of a covariant vector defined as shown in Fig. 1. For an orthogonal coordinate system, only the diagonal components will be nonzero [as shown as (1)]. Moreover, the contravariant and covariant components will be collinear in

Fig. 4.   Reconstruction of a "triangle" mesh.

Fig. 5.   (a) An oblique structure with a corner meshed by new FDTD method. (b) An oblique structure with a corner meshed by CPFDTD.

of the intercepted cell and its neighbors are moved, as shown in Fig. 4(b).

B. Reconstruction of Triangle Cells

The location of the new node positions are chosen as follows.

As we know, the coordinates of the two intercepted points—the equation of straight line $A'B'$ in Figs. 3 and 4—can be described as

$$\frac{x - m\delta x}{m\delta x - f^{-1}(n\delta z)} = \frac{z - f(m\delta x)}{f(m\delta x) - n\delta z}.$$

The middle point of segment $A'B'$ is

$$D': x_{D'} = \frac{m\delta x + f^{-1}(n\delta z)}{2}$$
$$z_{D'} = \frac{f(m\delta x) + n\delta z}{2}$$

and then the line which passes through D', which is perpendicular to $A'B'$, will be described as

$$z - z_{D'} = k(x - x_{D'})$$

where

$$k = -\frac{m\delta x - f^{-1}(n\delta z)}{f(m\delta x) - n\delta z}.$$

Then the additional point will be determined by the combination of the following two equations:

$$z = f(x), \qquad \text{curved material boundary}$$
$$z - z_{D'} = k(x - x_{D'}), \qquad \text{line } C'D'$$

Having performed the above steps, we obtain the new nonorthogonal FDTD meshes on the curved boundary for those triangular meshes. Fig. 2(c)–(e) can all be treated in a similar way as that given above. The reason for treating the curved boundary using the above method is summarized below.

1) Each row and column in the modified mesh has the same number of cells as the unmodified mesh, which simplifies the computer program.
2) The new nonorthogonal grids remain quadrilateral, and keep the basic characteristic of FDTD cells, which facilitates not only the central-difference approximation
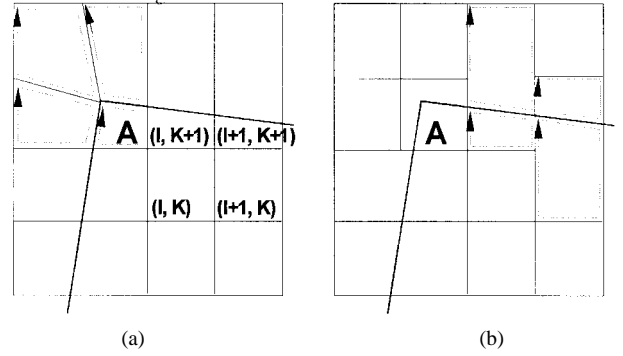
analog to the space derivative of the covariant and contravariant components of the electromagnetic field, but is a natural geometry for Faraday and Ampere's Laws in the nonorthogonal coordinate system as well.

3) The interface between cells modified using this scheme and other algorithms based on a Cartesian system (such as staircase and CPFDTD) is simple.

C. Treatment of Corners in Angular Objects

If oblique structures with corners such as a rotated rectangular disk [shown in Fig. 5(a)] are considered, the cell containing the corner can be treated as a "triangle"; but in this case, the extra node point is placed on the corner. By doing this, we have taken the position of the corners into consideration, which will improve the precision of the method. The example of an oblique rectangular disk modeling by CPFDTD is shown in Fig. 5(b), which shows that the small quadrilateral area A has not been taken into consideration in the CPFDTD mesh. This will introduce an inaccuracy if the mesh is coarse, which is avoided in the method described here.

D. Choosing the Position of the Nodes in Modified Cells

Once the new coordinates including those "triangle" and "flag" cells are determined, it is easy to set E and H nodes in each cells. We choose the middle points of nodes on the x- and z-axis, respectively, as E_x and E_z nodes for TE modes, and then the centroid of the cell as H nodes, which are similar to the traditional FDTD approach. The position of the node on the material boundary is then determined using the procedure described in Section III-B. In fact, x, y, and z cannot be regarded as Cartesian coordinates now. Those components of the electric field (for TE modes) and the magnetic field (for TM modes) on the interface of material are along the boundary. Therefore, these coordinates are generalized ones.

Once the node position of the electric and magnetic field are determined, the components of metric tensor g_{ij} in nonorthogonal cells can be calculated and stored [shown as (1)]. There is an approximation when we try to find out the tangential lines of the given curved boundary on every nodes. It is not easy to define them exactly when the equation of the material boundary is unknown. Usually if we use a chord, such as $A'C'$ or $C'B'$ in Fig. 4 to replace them, it will not cause a large error.

IV. FDTD ITERATION FORMULA IN NEW MESHES

In the previous section, the meshing of a curved boundary on the Cartesian coordinate system was defined. The conventional FDTD approach can then be used on those Cartesian cells, and nonorthogonal method can be used on those nonorthogonal cells, with the values exchanged on those common nodes.

As an example, consider the structure shown in Fig. 5(a). Cell (i, k) is a Cartesian cell, and we can use the traditional FDTD iteration formula [as shown as (2)] to obtain the E and H components. During iteration, covariant and contravariant components are not necessary, and, therefore, the memory requirements are the same as for standard FDTD:

$$
\begin{aligned}
E_x^{n+1}(i, k) &= E_x^n(i, k) - \frac{\delta t}{c\varepsilon_r \delta z} \\
&\quad \cdot [H_y^{n+1/2}(i, k) - H_y^{n+1/2}(i, k-1)] \\
E_z^{n+1}(i, k) &= E_z^n(i, k) + \frac{\delta t}{c\varepsilon_r \delta x} \\
&\quad \cdot [H_y^{n+1/2}(i, k) - H_y^{n+1/2}(i-1, k)] \\
H_y^{n+1/2}(i, k) &= H_y^{n-1/2}(i, k) + \frac{\delta t}{c\mu_r \delta x} \\
&\quad \cdot [E_z^n(i+1, k) - E_z^n(i, k)] \\
&\quad - \frac{1}{\mu_r \delta z}[E_x^n(i, k+1) - E_x^n(i, k)] \quad (2)
\end{aligned}
$$

where δx and δz are variable space steps given by

$$
\delta x = |x_{i+1} - x_i|
$$
$$
\delta z = |z_{j+1} - z_j|.
$$

Cell $(i, k+1)$ is nonorthogonal, so we use a nonorthogonal FDTD method to find the value of E and H components. The equations for this cell are

$$
\begin{aligned}
E^x&(i, k+1)^{n+1} \\
&= E^x(i, k+1)^n + \frac{\delta t}{c\varepsilon_r} \\
&\quad \cdot [H_y(i, k) - H_y(i, k+1)]^{n+1/2} \sqrt{\frac{1}{g^{yy}}} \cdot \sqrt{\frac{g_{xx}}{g}} \\
E^z&(i, k+1)^{n+1} \\
&= E^z(i, k+1)^n + \frac{\delta t}{c\varepsilon_r} \\
&\quad \cdot [-H_y(i, k+1) + H_y(i, k+1)]^{n+1/2} \sqrt{\frac{1}{g^{yy}}} \cdot \sqrt{\frac{g_{zz}}{g}} \\
H^y&(i, k+1)^{n+1/2} \\
&= H^y(i, k+1)^{n+1/2} + \frac{\delta t}{c\mu_r} \cdot \sqrt{\frac{g_{yy}}{g}} \\
&\quad \cdot \left[\frac{E_z(i+1, k+1)}{\sqrt{g^{zz}(i+1, k+1)}} - \frac{E_z(i, k+1)}{\sqrt{g^{zz}(i, k+1)}} \right. \\
&\quad \left. - \frac{E_x(i, k+2)}{\sqrt{g^{xx}(i, k+2)}} + \frac{E_x(i, k+1)}{\sqrt{g^{xx}(i, k+1)}} \right]^{n-1/2}. \quad (3)
\end{aligned}
$$

In the above equations, the contravariant components in cell (i, k) and $(i+1, k)$ need not be transformed into covariant components because in Cartesian cells they are collinear. In
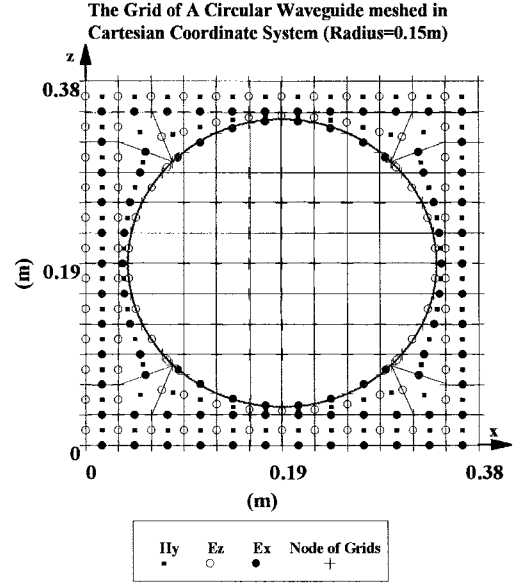

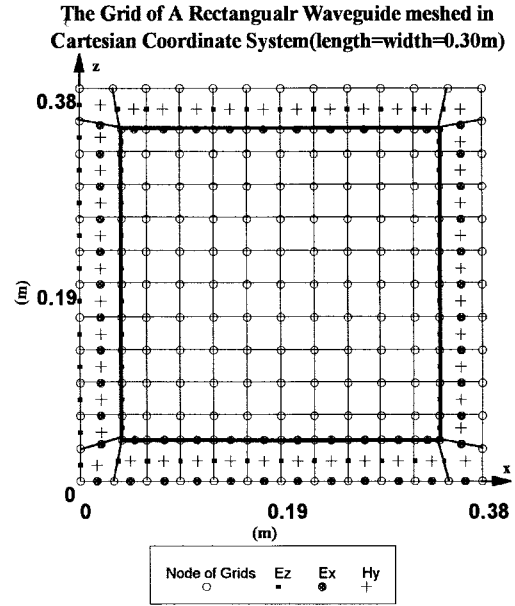Fig. 6. A circular waveguide meshed in Cartesian grids.

Fig. 7. A rectangular waveguide meshed in Cartesian grids.

nonorthogonal cells, transformation is necessary by use of

$$
\begin{aligned}
E_x(i, k+1) &= G_{xx} E^x(i, k+1) \\
&\quad + \frac{G_{xy}}{4} \left[E^z\left(i+\frac{1}{2}, k+1-\frac{1}{2}\right) \right. \\
&\quad + E^z\left(i-\frac{1}{2}, k+1-\frac{1}{2}\right) \\
&\quad + E^z\left(i+\frac{1}{2}, k+1+\frac{1}{2}\right) \\
&\quad \left. + E^z\left(i-\frac{1}{2}, k+1+\frac{1}{2}\right) \right] \\
H_Y(i, k+1) &= H^y(i, k+1) \\
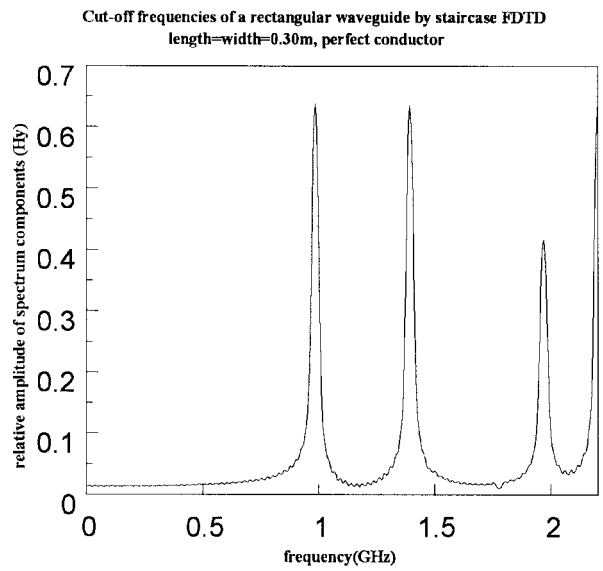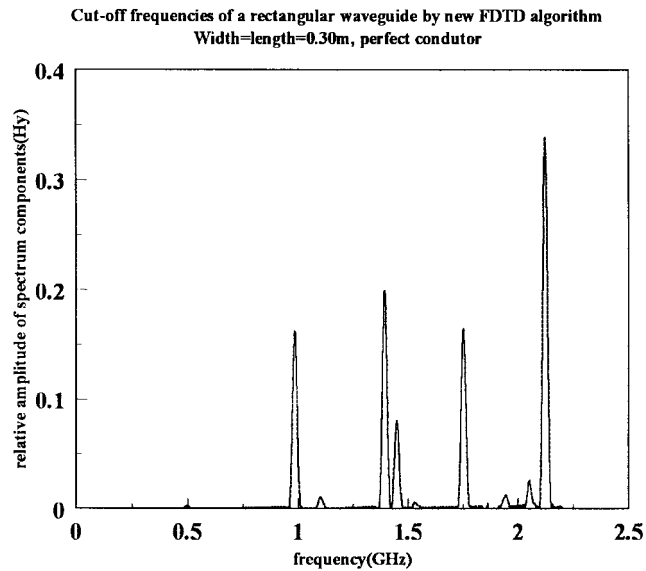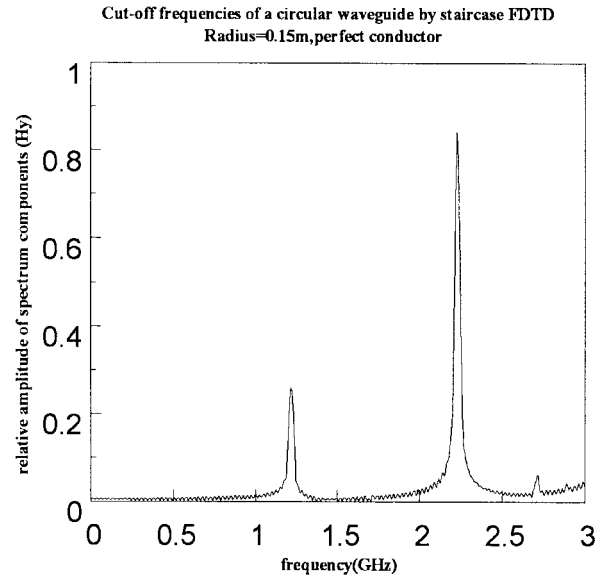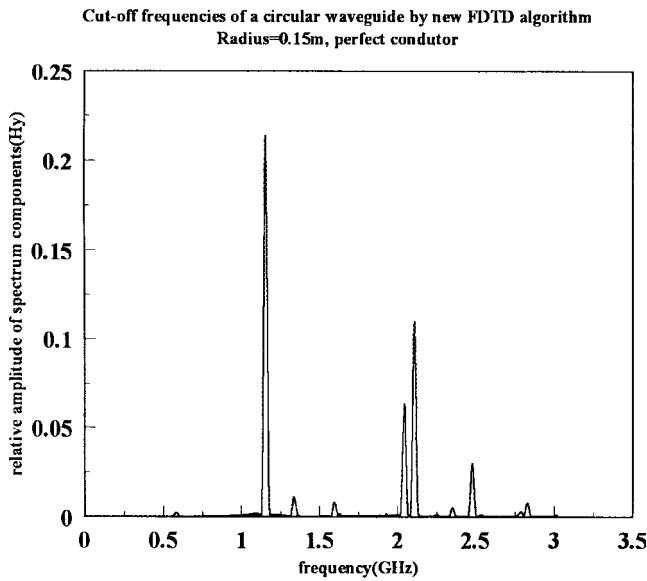G_{xz} &= \sqrt{\frac{g_{xx}}{g^{zz}}} \cdot g_{xz} \quad (4)
\end{aligned}
$$

Cut-off frequencies of a circular waveguide by new FDTD algorithm
Radius=0.15m, perfect condutor

Cut-off frequencies of a circular waveguide by staircase FDTD
Radius=0.15m, perfect conductor

Cut-off frequencies of a rectangular waveguide by new FDTD algorithm
Width=length=0.30m, perfect condutor

Cut-off frequencies of a rectangular waveguide by staircase FDTD
length=width=0.30m, perfect conductor

Fig. 8. The FFT of an Hy-field component by a new FDTD algorithm on waveguides.

Fig. 9. The FFT of an Hy-field component by a staircase algorithm on waveguides.

where x, y, and z denote generalized coordinates in nonorthogonal coordinate system, and will reduce to Cartesian coordinates in those Cartesian cells.

Figs. 6 and 7 show the grids of circular and rectangular waveguides which are generated by computer software. The region between the boundaries of each waveguide and the boundary of the computational domain is PEC. We find that most of cells are Cartesian, where a Cartesian cell is defined as being rectangular and which can be treated using standard FDTD—only those near the boundaries are nonorthogonal. Not every E and H node is shown in the figures, only those outside the metal are given. The boundary condition for a PEC dictates that those E nodes on and outside boundaries are zero. It can be seen that electric- and magnetic-field components satisfy the boundary condition precisely in the new FDTD scheme and no approximation need be made. It will also ensure that fewer

cells are needed in this scheme than in others, and it will be powerful when some scattering problem with small scatterings are considered. An example can be given to illustrate the computer resources saved due to this new method. For a circular waveguide meshed in a 6 × 6 computational region, there are 32 nonorthogonal cells and four Cartesian cells. If a circular waveguide with the same dimensions is taken into consideration [i.e., in a 12 × 12 computational region (as shown in Fig. 6)] there are 64 nonorthogonal cells and 80 Cartesian cells. Therefore, the new method is very efficient in computation of an electromagnetic scattering problem. The more fine grids there, the more efficient the new method.

V. NUMERICAL RESULTS

In order to demonstrate the propriety of the new FDTD method, some numerical results are presented. The cutoff

TABLE I
NUMERICAL RESULTS ON A CIRCULAR WAVEGUIDE AND ITS COMPARISON TO THE THEORETICAL RESULTS

new FDTD	CPFDTD	Theoretical	new FDTD(%)	CPFDTD(%)
0.5720	0.5666	0.5863	-2.44	-3.36
0.9397	--	0.9721	-3.33	–
1.1849	1.1767	1.2198	-2.86	-3.53
1.3687	1.3045	1.3372	+2.36	-2.45
1.6343	1.5980	1.6930	-3.47	-5.61
1.7365	1.7142	1.700	+2.15	+0.84
1.9612	--	2.043	-1.96	--
2.1042	2.1355	2.136	-1.49	0.00
2.2063	--	2.234	-1.24	--
2.3493	--	2.389	-1.66	--
2.5332	2.5133	2.553	-0.78	-1.56
2.7784	2.6004	2.718	+2.22	-4.33
2.7784	2.7893	2.732	+1.70	+2.10
3.0031	2.8910	2.956	+1.59	-2.20

TABLE II
NUMERICAL RESULTS ON A RECTANGULAR WAVEGUIDE AND ITS COMPARISON TO THE THEORETICAL RESULTS

new FDTD	CPFDTD	Theoretical	new FDTD(%)	CPFDTD(%)
0.4968	0.4976	0.500	-0.64	-0.48
0.7039	--	0.707	0	–
0.9908	0.9842	1.000	-0.92	-1.58
1.1139	1.1404	1.118	-0.37	+2.00
1.3994	1.3982	1.414	-1.03	-1.12
1.5216	1.5363	1.500	+1.44	+2.42
1.6458	1.6687	1.581	+4.10	+5.55
1.7700	1.8886	1.803	-1.67	+4.92
1.9460	--	2.000	-2.70	--
2.0391	--	2.062	-1.11	--
2.1323	2.0847	2.121	+0.53	-1.71

TABLE III

	CPU Time (16 384 steps)	The Required Memory for Metric Tensors
Nonorthogonal FDTD	35.1 s	19 152 byte
This New Algorithm	23.2 s	8502 byte

frequencies of the circular waveguide and the rectangular waveguide shown in Figs. 6 and 7, respectively, have been calculated. The computational region is 0.38×0.38 m^2 meshed by 12×12 nodes. The time step is obtained as

$$\Delta t \leq \frac{1}{c} \cdot \min \left(\frac{\sqrt{g}}{\sqrt{g_{11} + g_{22} - 2g_{12}}} \right).$$

Fig. 8 shows the simulation results by performing fast Fourier transform (FFT) of the time-domain signal on circular and rectangular waveguides, respectively. The values of cutoff frequencies are listed in Tables I and II. Fig. 9 shows the responding results by staircase FDTD for the same computational region; however, a more dense grid comprising 60×60 cells is used. Not all the modes are able to be determined by a probe at a single position on the waveguide. If we choose few cells in the staircase approach, spurious modes will appear because of numerical dispersion.

Tables I and II show the list of numerical results obtained using the new method CPFDTD, utilizing the same number of cells and some theoretical results. Agreement is good with the errors not exceeding 5%. It can be seen that for the CPFDTD method, some modes are not seen when a 12×12 grid is used, and slightly higher errors occur for the simulation of a rectangular waveguide. The reason is that the singular points at the corners of the rectangle are not taken into account in the CPFDTD approach. All simulations have been performed on an HP workstation (Apollo-700). We compare this new algorithm with a nonorthogonal FDTD method with the CPU time and the required memory to store the metric tensors, with results (for a circular waveguide simulation excluding mesh generation) shown in Table III.

VI. CONCLUSION

This paper has introduced a new FDTD scheme which is based on using a nonorthogonal FDTD algorithm (so as to deal with an arbitrary electromagnetic structure on an underlying Cartesian grid). This has the benefit of reduced computer resources and easily generated meshes. This arrangement of field nodes also allows existing FDTD algorithms, which have been developed for a Cartesian coordinate system, to be immediately incorporated into a new FDTD program.

These include absorbing boundary conditions and near–far field transformations. A further advantage of the new FDTD scheme is that it reduces to conventional FDTD codes when those structures to be studied are simple rectangles. Numerical simulation shows that the new method is very efficient and results agree very well with theoretical ones. We believe that it will be more powerful in computation of the electromagnetic scattering problem. The application and extension of the method to those electromagnetic structures (in three dimensions with dielectric boundaries) have been studied and their results will soon be announced.

ACKNOWLEDGMENT

REFERENCES

[1] K. S. Yee, "Numerical solution of initial boundary value problems involving Maxwell's equations in isotropic media," *IEEE Trans. Antennas Propagat.,* vol. AP-14, pp. 302–307, May 1966.

[2] A. C. Cangellaris and D. B. Wright, "Analysis of the numerical error caused by the stair-stepped approximation of a conducting boundary in FDTD simulations of electromagnetic phenomena," *IEEE Trans. Antennas Propagat.,* vol. 39, pp. 1518–1525, Oct. 1991.

[3] T. G. Jurgens, A. Taflove, K. Umashankar, and T. G. Moore, "Finite-difference time-domain modeling of curved surfaces," *IEEE Trans. Antennas Propagat.,* vol. 40, pp. 357–366, Apr. 1992.

[4] T. G. Jurgens and A. Taflove, "Three-dimensional contour FDTD modeling of scattering from single and multiple bodies," *IEEE Trans. Antennas Propagat.,* vol. 41, pp. 1703–1708, Dec. 1993.

[5] C. J. Railton, I. J. Craddock, and J. B. Schneider, "Improved locally distorted CPFDTD algorithm with provable stability," *Electron. Lett.,* vol. 31, no. 18, Aug. 1995.

[6] C. J. Railton and I. J. Craddock, "A modified CPFDTD algorithm for the analysis of arbitrary 3D PEC structures," *Proc. Inst. Elect. Eng.,* pt. H, vol. 143, pt. H, no. 5, pp. 367–372, Oct. 1966.

[7] R. Holland, "Finite difference solutions of Maxwell's equations in generalized nonorthogonal coordinates," *IEEE Trans. Nucl. Sci.,* vol. NS-30, pp. 4589–4591, 1983.

[8] J. A. Stratton, *Electromagnetic Theory.* New York: McGraw-Hill, 1941, pp. 38–47.

[9] R. Holland, "A finite difference time-domain EMP code in 3-D spherical coordinates," *IEEE Trans. Nucl. Sci.,* vol. NS-30, pp. 4592–4595, 1983.

[10] M. Fusco, "FDTD algorithm in curvilinear coordinates," *IEEE Trans. Antennas Propagat.,* vol. 38, pp. 76–89, Jan. 1990.

[11] J. F. Lee, R. Palandech, and R. Mittra, "Modeling three-dimensional discontinuities in waveguides using nonorthogonal FDTD algorithm," *IEEE Trans. Microwave Theory Tech.,* vol. 40, pp. 346–352, Feb. 1992.

[12] P. H. Harms, J. F. Lee, and R. Mittra, "A study of the nonorthogonal FDTD method versus the conventional FDTD technique for computing resonant frequencies of cylindrical cavities," *IEEE Trans. Microwave Theory Tech.,* vol. 40, pp. 741–746, Apr. 1992.

[13] B. Singh and A. C. Marvin, "Hybrid finite-volume finite-difference time-domain modeling of curved surfaces," *Electron. Lett.,* vol. 31, no. 5, Mar. 1995.

Yang Hao received the B.S. degree from Shandong University and the M.S.E. degree from Nanjing Research Institute of Electronics Technology (NRIET), China, in 1989 and 1992, respectively, and is currently working toward the Ph.D. degree in electrical and electronic engineering at the Centre for Communications (CCR), University of Bristol, Bristol, U.K.

From 1992 to 1995, he was an R&D Engineer at NRIET, working on antenna and microwave integrated circuits. His research interests include numerical methods in electromagnetics and microwave integrated circuits, and antenna design.

Chris J. Railton (M'88) received the B.Sc. degree in physics from the University of London, London, U.K., in 1974 and the Ph.D. degree in electronic engineering from the University of Bath, Bath, U.K., in 1988.

From 1974 to 1984, he worked with the Scientific Civil Service on a number of research and development projects in the areas of communications, signal processing, and electromagnetic compatibility (EMC). From 1984 to 1987, he worked at the University of Bath on the mathematical modeling of boxed microstrip circuits. He is currently with the Centre for Communications Research (CCR), University of Bristol, Bristol, U.K., leading the Computational Electromagnetics Group, which is involved in the development of new algorithms and their application to MMIC's, planar antennas, microwave and RF heating, EMC, and high-speed logic.